

Geometric Accuracy Analysis of Stationary BTF Gonioreflectometers

Vlastimil Havran

Faculty of Electrical Engineering, Czech Technical University in Prague, Czech Republic

Abstract

The accurate BTF data representation requires specialized measurement gantries, some of them designed as gonioreflectometers. These consist of an illumination source and a camera mounted on two robotic arms, one degree of freedom possibly achieved by rotation stage which a measured sample is mounted on. While there are several variations of the gonioreflectometer gantry, the principle of all remains the same, positioning directly the illumination and detector on a hemispherical surface over a sample. We analyze the positioning error of such gonioreflectometers. The input parameters are the required spatial resolution of a BTF sample and the distance between the camera used as a detector and the BTF sample. Our analysis confirms that the requirements for mechatronic actuators for the positioning of the sample and arms are very high and near the limit of state of the art technology.

Categories and Subject Descriptors (according to ACM CCS): I.3.7 [Computer Graphics]: Three-Dimensional Graphics and Realism—Color, shading, shadowing, and texture I.4.1 [Image Processing and Computer Vision]: Digitization and Image Capture—Reflectance

1. Introduction

A possibility to use Bidirectional texture function (BTF) as means of the surface reflectance representation has been around more than last 15 years since the introductory article by Dana et al. [DVGNK99]. It can be used in various scientific disciplines dealing with visual appearance of surfaces including computer graphics, computer vision, design etc. It extends the formalization of surface reflectance known as *bidirectional reflectance distribution function* (BRDF) [NRH*77]. BRDF under some ideal assumptions that are nearly impossible for a physical realization (measuring a surface reflectance for a single point) exhibits two important physical laws: Helmholtz reciprocity and energy conservation. Surface reflectance representation by BTF breaks potentially the two laws and allows for capturing various subtle effects occurring at macro scale level (roughly resolving power 2 to 20 lines per mm), such as self-shadowing, masking and subsurface scattering. There are in general four categories of BTF gantries used to acquire BTF data for stationary based setups: gonioreflectometer based setups, mirror and kaleidoscope setups, camera and light array setups, and possibly other remaining designs, such as

using ellipsoid semitransparent mirror with moving X-Y stage [Dan01]. BTF gantries were surveyed recently by Schwartz et al. [SSW*14].

In our paper we focus on BTF gonioreflectometer based setups. While our analysis is also valid for other construction categories of BTF gantries, though it could be easier to compute the compensation by precalibration. We start from the camera resolution, the camera lens and the distance to the sample and analyze the requirements on angular positioning accuracy for the motion actuators used for robotic arms. We show that for a reasonable gonioreflectometer design it is possible to achieve required angular accuracy of positioning with the most accurate technology used for positioning.

2. Related Work

Below we shortly describe the most important work based on BTF gantries using gonioreflectometers. A setup based on robotic arms used to acquire BRDF datasets was used already in early sixties and seventies. An example of such a setup used in computer graphics is the one built up at Cornell University, described in more detail in [Foo97]. The gonioreflectometer was also used in pioneering work of Dana

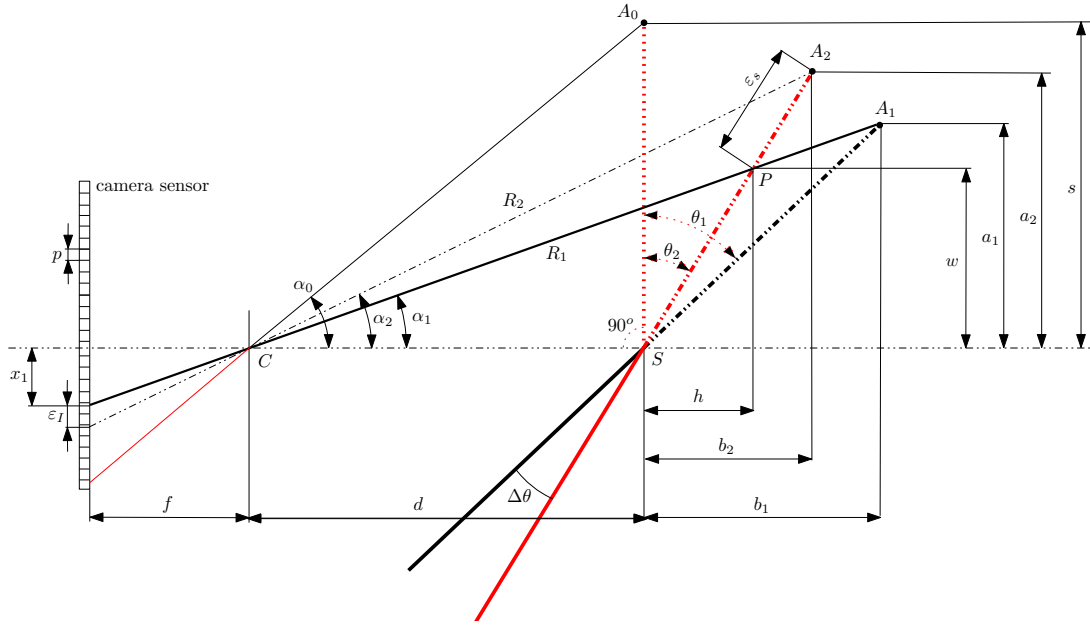


Figure 1: Geometric situation to evaluate a positioning error for incorrectly rotating the robotic arm by error angle $\Delta\theta$ over the sample of size $2s$ centered at point S , when viewed by a pinhole camera from distance d and with lens of focal length f , using a camera sensor with a pixel size p .

et al. [DVGNK99], where one degree of freedom was oriented manually and the three by a robotic arm. Another setup was built by Sattler et al. [SSK03] at the University of Bonn, where a sampler holder is put onto the robotic arm with 3 degrees of freedom, the illumination source is fixed in space and the camera is moving along a semicircle-rail-system. An Intellitel SCORBOT-ER 4u robot arm is used to position and orientate the sample holder, achieving for three degrees of freedom. This gantry was revised to use another camera [MMS*04] and later to allow for spectral measurements [RSK10]. More recent gonioreflectometer BTF gantry was described by Filip et al. [FVH*13], where a sample holder is mounted on a rotating stage, the camera moves with one degree of freedom, and a light source by two other degrees of freedom. Another interesting BRDF gonioreflectometer based setup achieving a high accuracy measurement was described by Huenerhoff et al. [HGH06]. This setup uses an accurate robot with 5-degrees of freedom for a sampler holder and a large rotational stage for moving the light source while the camera is fixed.

From the work related to surface normal orientation for BRDF and BTF let us mention the two contributions. Magnor [Mag03] studied the change of BRDF when changing the normal orientation. The method to estimate a correct sample plane during the BTF measurement to allow for images registration was proposed by Vávra and Filip [VF12], considering incorrect tilt of a sample normal to the plane with registration marks used in BTF gantry.

In general, all the described gonioreflectometers follow the same principle - a light source and a camera move around the measured sample along a hemisphere. Possibly, some BRDF gonioreflectometer based setups are simplified as they are designed only for isotropic surfaces. Most of existing BRDF gonioreflectometers could be redesigned to acquire BTF data as well, by changing the detector to camera and possibly changing the light source.

3. Analysis Background

Due to mechanical play of any setup, each captured image has its own and unique coordinates for positioning both camera and illumination source. We want to analyze the required accuracy and repeatability of positioning the camera with respect to a sample with three applications:

- accuracy of measurement with respect to the positioning of a sample, which is important for highly glossy surfaces, in particular to the peak of a specular lobe,
- the opposite task - the required accuracy of positioning the sample in a BTF gantry, assuming the measured sample is nearly flat,
- necessity to compute the individual registration of all captured images or not, when the registration using only pre-computed data could be applied. In case of high reproducibility of a camera and a light source positions along hemisphere the individual registration is not needed.

Our analysis starts from a simple geometric consideration as shown in Figure 1. A camera equipped with an ideal lens and

CCD/CMOS camera sensor is at a specific distance d from the measured sample. We assume that the direction between the sample center $(0,0,0)$ and robotic arm holding the camera is parameterized by d, θ , and φ in spherical coordinate system $(x, y, z) = (d \sin \theta \cos \varphi, d \sin \theta \sin \varphi, d \cos \theta)$.

We can evaluate the effect of angular error positioning of an arm to the angle θ_2 instead of the correct angle θ_1 over the sample twofolds:

- *in object space on a sample* - the error shift ϵ_S of a point on the sample as being seen on the camera chip for the same pixel, while a pixel on a camera remains the same,
- *in image space on a camera sensor* - the error shift ϵ_p of a point on a camera sensor from the right position to a wrong position.

For the derivations of errors in two spaces we will need the following terms as shown in Figure 1:

- distance d between the camera and the sample,
- focal length f of the camera,
- size of pixel p on the camera detector,
- size $2s$ of BTF sample.

4. Object Space Error Analysis

For this analysis we consider a ray R_1 from a pixel x_1 through the lens center. That pixel in the object space corresponds either to the point A_1 for correct rotational positioning of a sample at an inclination angle $\angle \theta_1$, while in reality the sample is rotated at an inclination angle $\angle \theta_2$, hence the point P is being viewed at the camera pixel x_1 . We want to compute the error ϵ_S as the distance between the point A_1 and the point P as a result of the inclination angle error $\Delta \theta = \theta_2 - \theta_1$. We can start the derivation from a simple trigonometric functions and property of similar triangle:

$$a_1 = s \cos \theta_1, \quad a_2 = s \cos \theta_2 \quad (1)$$

$$b_1 = s \sin \theta_1, \quad b_2 = s \sin \theta_2 \quad (2)$$

$$\frac{a_1}{d+b_1} = \frac{w}{d+h}, \quad \frac{a_2}{b_2} = \frac{w}{h} \quad (3)$$

Then we can compute unknown positions of a point $P = (w, h)$ for incorrectly rotated sample at angle θ_2 as follows:

$$w = \frac{da_1a_2}{a_2(d+b_2) - a_1b_2} \quad (4)$$

$$h = \frac{da_1b_2}{a_2(d+b_2) - a_1b_2}, \quad (5)$$

so the error $\epsilon_{S,\theta}$ between the right point A_1 and incorrectly considered point P :

$$\epsilon_{S,\theta}[mm] = \sqrt{(h-b_2)^2 + (w-a_2)^2} \quad (6)$$

or alternatively this can be expressed by using either trigonometric function $\sin \theta_1$ or $\cos \theta_1$:

$$\epsilon_{S,\theta}[mm] = \frac{b_2 - h}{\sin \theta_1} = (b_2 - h) \frac{s}{b_2} = \frac{a_2 - w}{\cos \theta_1} = (a_2 - w) \frac{s}{a_2} \quad (7)$$

Substituting for terms a_1, a_2, b_1 and b_2 we get then in terms of s, θ_1, θ_2 and d this error:

$$\epsilon_{S,\theta} = s \left(\cot \theta_2 - \frac{d \cos \theta_1 \cot \theta_2}{\cos \theta_2 (d + s \sin \theta_2) - \cos \theta_1 s \sin \theta_2} \right) \quad (8)$$

For small changes in azimuth angle $\varphi = \varphi_1 - \varphi_2$ (assuming $\sin \alpha = \alpha$), so instead of correct angle φ_1 using φ_2 , we get the error of positioning the sample simply as:

$$\epsilon_{S,\varphi}[mm] \approx s \cos \theta_1 \sin(\varphi_2 - \varphi_1) \quad (9)$$

Putting the two errors together we then get the total error ϵ_S for both inclination and azimuthal error as follows:

$$\epsilon_S[mm] \approx \sqrt{\epsilon_{S,\theta}^2 + \epsilon_{S,\varphi}^2} \quad (10)$$

5. Image Space Error Analysis

The image space error analysis requires to compute the error in camera coordinate space on a camera sensor. The error due to wrong inclination of camera with respect to the sample on a camera sensor is simply computed as:

$$\frac{a_1}{d+b_1} = \frac{x_1}{f}, \quad \frac{a_2}{d+b_2} = \frac{x_2}{f} \quad (11)$$

$$\epsilon_{I,\theta}[mm] = \frac{fa_1}{d+b_1} - \frac{fa_2}{d+b_2} \quad (12)$$

When we substitute for a_1, a_2, b_1 , and b_2 and compute the distance between individual pixels of size p , we get then the error in image space expressed in pixels as:

$$\epsilon_{I,\theta}[-] = \frac{\epsilon_{I,\theta}[mm]}{p} = \frac{1}{p} \left(\frac{fs \cos \theta_1}{d + s \sin \theta_1} - \frac{fs \cos \theta_2}{d + s \sin \theta_2} \right) \quad (13)$$

In azimuthal plane for using φ_2 instead of correct φ_1 we compute the error as distance on the camera sensor as:

$$\epsilon_{I,\varphi}[mm] = \frac{fa_1}{d+b_1} \sin(\varphi_2 - \varphi_1) = \frac{fs \cos \theta_1 \sin(\varphi_2 - \varphi_1)}{d + s \sin \theta_1} \quad (14)$$

and in terms of pixels then:

$$\epsilon_{I,\varphi}[-] = \frac{\epsilon_{I,\varphi}[mm]}{p} = \frac{fs \cos \theta_1 \sin(\varphi_2 - \varphi_1)}{p(d + s \sin \theta_1)} \quad (15)$$

Putting the two pixel errors together we then get the total error ϵ_I for both inclination and azimuthal error as follows:

$$\epsilon_I \approx \sqrt{\epsilon_{I,\theta}^2 + \epsilon_{I,\varphi}^2} \quad (16)$$

6. Analysis of Existing BTF Gonioreflectometers

We can utilize the known data about the construction and properties of existing BTF gantries to compute the error in object and image space. Based on the error we can determine if all the captured images have to be registered individually when rectifying the images prior further processing, such as BTF data compression. In Table 1 we summarize the already described important properties of existing BTF/BRDF gonioreflectometers plus the maximum inclination angle θ_{max} used for measurement and the found angular error $\Delta \theta, \Delta \varphi$

Described at		Gonioreflectometer specification					#5 (BRDF) [HGH06]
		#1 [SSK03]	#2 [MMS*04]	#3 [RSK10]	#4 [FVH*13]		
Distance d	mm	1700	1700	2400	2000	781.84	
Focal length f	mm	180	180	135	180	-	
Camera model		Kodak DCS 760	Kodak DCS Pro 14n	CoolSNAP K4	AVT Spike 1600 C	-	
Sensor size	mm	27.65×18.48	36×24	15.155×15.155	36×24	-	
Pixels	-	3072×2048	4560×3048	2048×2048	4872×3248	-	
Pixel size p	μm	9×9	7.8×7.8	7.4×7.4	7.4×7.4	-	
Half sample size s	mm	40	40	32.5	70	-	
Max. inclination θ_{max}	$^{\circ}$	75	75	85	75	88	
Angular error $\Delta\theta$ and $\Delta\phi$	$^{\circ}$	$\pm 0.61^*$	$\pm 0.61^*$	$\pm 0.61^*$	± 0.03	± 0.002	
Object space error $\varepsilon_{S,\theta}$	[mm]	1.56	1.56	4.40	0.080	-	
Object space error $\varepsilon_{S,\phi}$	[mm]	0.11	0.11	0.04	0.005	-	
Object space error ε_S	[mm]	1.56	1.56	4.40	0.080	-	
Image space error $\varepsilon_{I,\theta}$	[pixels]	4.73	5.46	3.17	0.242	-	
Image space error $\varepsilon_{I,\phi}$	[pixels]	1.26	1.46	0.28	0.065	-	
Image space error ε_I	[pixels]	4.90	5.65	3.18	0.250	-	

Table 1: The summary of properties for existing BTF gantries and one BRDF gantry based on gonioreflectometer construction. Note that the last column belongs to BRDF gantry that was designed for metrological applications. * The accuracy in angle positioning for UBO gantry was only estimated from the robot documentation as it is not clearly specified there, but given in numbers from measurement in [SSW*14].

of arm positioning. The object space and image space error are then computed according to the formulas derived in the previous section.

From the results in Table 1 it is apparent that for original camera resolution the object space error is rather big as viewing at the inclination angle 75° or even 85° would require extremely accurate positioning to keep the error below acceptable level. Fortunately, as the footprint of the sample on the camera sensor decreases with $\cos\theta$ factor as well, the image space error remains at acceptable level for designs #4, while the images acquired from gantries #1 to #3 require careful image registration based on the registration marks that are close to BTF sample. The dependence of an object space and image space error on the inclination angle θ for gantries #1 to #4 is shown in graph in Figure 2.

Discussion. The object space error ε_S depends on the inclination angle θ , the higher the angle θ the larger the object space error. The image space error ε_I almost does not depend on the inclination angle θ and only increases with the angular error $\Delta\theta$ and $\Delta\phi$ of arm positioning. To keep the image space error in a reasonable range (such as $\varepsilon_I < 0.25$) for easy subsequent image data processing we need to have sufficiently accurate and reproducible positioning of arm with the angle positioning error below $0.03^{\circ} = 1.8$ arc minutes. This way we can avoid the individual registration of each captured image as we can use precomputed data for registration. If the angular positioning error is high, it is necessary to compute image registration for each captured image individually, based on detection of registration marks attached to the BTF sample or a sample holder, as described for the

gantries #1 to #3 in [SSK03, MMS*04, RSK10]. The individual image registration cannot change the fact that data are measured at different four dimensional coordinates than specified, which can be important for glossy materials.

7. Consideration for future BTF gantries

While the camera/light source arrays may be seen as more perspective way of measuring BTF, they have two disadvantages: (1) the higher price, due to necessity to have several cameras and many light sources positioned on a hemisphere, (2) the impossibility to measure surface reflectance at some specified angles that might be required for some glossy BTF materials. The kaleidoscope BTF gantries [HP03] are of limited spatial and directional resolution. Therefore a BTF gonioreflectometer that needs only a single camera with lens, one light source, and only 4 degrees of freedom angular positioning mechanism seems to be the most economical way to acquire BTF data if we can accept longer acquisition times and/or we have low budget to build a BTF gantry.

We have checked the possibility of mechatronic actuators on the market to implement accurate rotational motion required by gonioreflectometers. To keep the error of angular positioning low enough it is necessary to use an accurate servo motor actuators featuring the absolute encoder with high number of bits per revolution. Current industrial production in theory allows to use such encoder up to 18 or 20 bits per shaft revolution, while in practice the absolute accuracy of these encoders is a bit lower and achieves maximally 14 to 16 bits. More difficult problem is that to allow for sufficient torque to move relatively rigid robotic arms with a

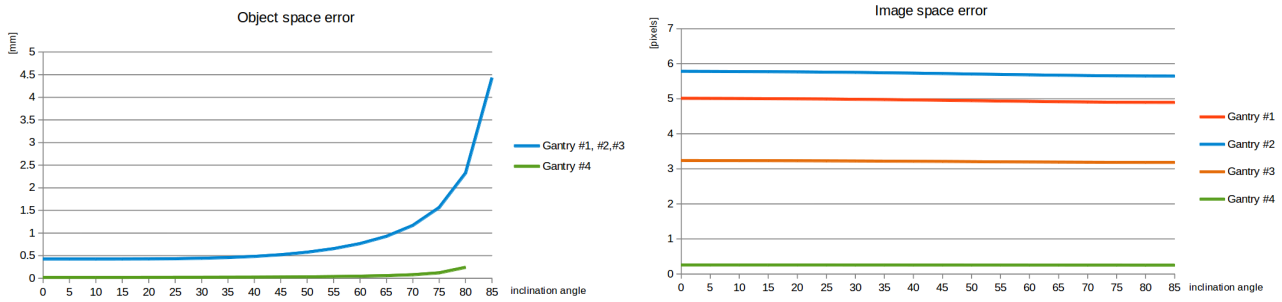


Figure 2: (left) Object space error in millimeters and (right) image space error in pixels for 4 existing BTF gantries described in Table 1 in dependence on the inclination angle θ .

load requires to use gear boxes that show a low backlash, i.e. angular error of rotational positioning. Figures in Table 1 indicate that only accurate harmonic gear boxes used in industrial robots with so called zero backlash would fulfill the high positioning accuracy requirements of BTF gantries, even if they have some hysteresis for motion and obviously non-zero torsional rigidity. Last but not least, it is necessary to compute how rigid is the arm of relatively big length up to 2000mm for a gonioreflectometer, if it holds a camera, heavy (telephoto) lens, and possibly a spectral filter in front of a lens. The design of these components (servo motor, gear box, arm length and weight and rigidity, the load on the arm) is interconnected and has to be carefully computed in mechanical design of BTF gonioreflectometer.

8. Conclusions

In this paper we have derived the error due to limited angular accuracy of moving arm for BTF gantry acquisition in both objects space on a sample and in image space on a camera detector. We have computed these errors for existing BTF gonioreflectometers. Further, we have discussed what are the consequences for possible future gonioreflectometers that could be constructed in case the BTF gantry has a limited financial budget for construction, if the acquired images should meet some image quality and possibly avoiding individual image registration for each image captured.

Acknowledgement

This research was partially supported by the Czech Science Foundation under project GA14-19213S and the Grant Agency of the Czech Technical University in Prague, grant No. SGS13/214/OHK3/3T/13. Further, I would like to thank Šárka Němcová for her comments on the paper manuscript.

References

[Dan01] DANA K.: BRDF/BTF Measurement Device. In *Computer Vision, 2001. ICCV 2001. Proceedings. Eighth IEEE International Conference on* (2001), vol. 2, pp. 460–466 vol.2. 1

- [DVGK99] DANA K., VAN-GINNEKEN B., NAYAR S., KOENDERINK J.: Reflectance and Texture of Real World Surfaces. *ACM Transactions on Graphics (TOG)* 18, 1 (Jan 1999), 1–34. 1, 2
- [Foo97] FOO S. C.: *A Gonioreflectometer For Measuring The Bidirectional Reflectance Of Material For Use In Illumination Computation*. Master's thesis, Cornell University, 1997. 1
- [FVH*13] FILIP J., VAVRA R., HAINDL M., ZID P., KRUPICKA M., HAVRAN V.: BRDF Slices: Accurate Adaptive Anisotropic Appearance Acquisition. In *In proceedings of the 26th IEEE Conference on Computer Vision and Pattern Recognition, CVPR 2013* (June 2013), pp. 4321–4326. 2, 4
- [HGH06] HUENERHOFF D., GRUSEMANN U., HOPE A.: New robot-based gonioreflectometer for measuring spectral diffuse reflection. *Metrologia* 43, 2 (2006), S11. 2, 4
- [HP03] HAN J. Y., PERLIN K.: Measuring Bidirectional Texture Reflectance with a Kaleidoscope. *ACM Trans. Graph.* 22, 3 (July 2003), 741–748. 4
- [Mag03] MAGNOR M. A.: Sensitivity of reflected radiance to surface normal orientation. In *ICIP (3)* (2003), pp. 717–720. 2
- [MMS*04] MÜLLER G., MESETH J., SATTLER M., SARLETTE R., KLEIN R.: Acquisition, Synthesis and Rendering of Bidirectional Texture Functions. In *Eurographics 2004, State of the Art Reports* (September 2004), Schlick C., Purgathofer W., (Eds.), INRIA and Eurographics Association, pp. 69–94. 2, 4
- [NRH*77] NICODEMUS F. E., RICHMOND J. C., HSIA J. J., GINSBERG I. W., LIMPERIS T.: *Geometric Considerations and Nomenclature for Reflectance*. Monograph 161, National Bureau of Standards (US), October 1977. 1
- [RSK10] RUMP M., SARLETTE R., KLEIN R.: Groundtruth Data for Multispectral Bidirectional Texture Functions. In *CGIV 2010* (June 2010), Society for Imaging Science and Technology, pp. 326–330. 2, 4
- [SSK03] SATTLER M., SARLETTE R., KLEIN R.: Efficient and Realistic Visualization of Cloth. In *Proceedings of the 14th Eurographics workshop on Rendering* (Aire-la-Ville, Switzerland, Switzerland, 2003), EGRW '03, Eurographics Association, pp. 167–177. 2, 4
- [SSW*14] SCHWARTZ C., SARLETTE R., WEINMANN M., RUMP M., KLEIN R.: Design and Implementation of Practical Bidirectional Texture Function Measurement Devices Focusing on the Developments at the University of Bonn. *Sensors* 14, 5 (2014), 7753–7819. 1, 4
- [VF12] VAVRA R., FILIP J.: Registration of Multi-View Images of Planar Surfaces. In *Proceedings of the 11th Asian Conference on Computer Vision, ACCV* (Nov 2012). 2